Classical density functional theory: an ideal tool to study heterogeneous crystal nucleation

Classical density functional theory: an ideal tool to study heterogeneous crystal nucleation

Gerhard Kahl[1] and Hartmut Löwen[2]

[1] Institut für Theoretische Physik and Center for Computational Materials Science (CMS),
Technische Universität Wien, Wiedner Hauptstraße 8-10, A-1040 Wien, Austria
[2] Institut für Theoretische Physik II, Weiche Materie, Heinrich-Heine-Universität Düsseldorf,
D-40225 Düsseldorf, Germany

E-mail: gkahl@tph.tuwien.ac.at

Abstract
Density functional theory provides an ideal microscopic theory to address freezing and
crystallization problems. We review the application of static density functional theory for the
calculation of equilibrium phase diagrams. We also describe the dynamical extension of density
functional theory for systems governed by overdamped Brownian dynamics. Applications of
density functional theory to crystallization problems, in particular to heterogeneous crystal
nucleation and subsequent crystal growth, are summarized. Heterogeneous nucleation at an
externally imposed nucleation cluster is discussed in detail, in particular for a simple
two-dimensional dipolar system. Finally the relation of dynamical density functional theory and
the phase field crystal approach are outlined.

(Some figures in this article are in colour only in the electronic version)

1. Introduction

Crystal growth processes are of high relevance for a variety of different problems ranging from crystallization of proteins [1] and other biological macromolecules [2] over the construction of photonic crystals with an optical bandgap [3] to applications in, for example, metallurgy [4]. A full microscopic understanding of crystal growth with the interparticle interactions and the thermodynamic boundary conditions as the only input is still a great challenge since it requires a microscopic theory of freezing. In this contribution we discuss how two successful concepts, namely classical density functional theory (DFT) and the phase field crystal (PFC) method, can be applied to solve this problem in a highly satisfactory way.

Investigations in recent years in (soft) condensed matter have given unambiguous evidence that (static) DFT is a very versatile and powerful tool to study the structural and thermodynamic properties of a wide variety of spatially inhomogeneous systems (for an overview we refer to [5, 6]). This refers, for instance, to fluids in different geometries of confinement [7], interfacial problems, such as surface

melting [8] or fluid interfaces, or crystallization, homogeneous liquid–gas nucleation [9] to name a few. In this contribution we focus on the phenomenon of crystallization. Starting from the interparticle potential, $\Phi(r)$, and the fluid correlations as an input, classical DFT is able to predict the crystallization transition and the full crystal structure. We will also give evidence that static DFT in combination with its dynamical extension, the so-called dynamic DFT (DDFT), represent ideal tools to study also heterogeneous crystal nucleation.

On the other hand, the PFC method has turned out to be highly successful in a broad variety of problems, such as interfaces [10], polycrystalline pattern formation [11, 12], or crystal nucleation and growth (see, e.g., [13–16]) to name a few. First developed by Elder and co-workers [17, 18] it is an extension of the phase field theory [19], suitably generalized to a situation with a crystal order parameter.

This contribution is structured as follows. In section 2 we provide a summary of the most relevant features of the concept of classical DFT, including a short overview over the commonly used density functionals, as well as a brief introduction into DDFT. Section 3 is dedicated to an outline of how to study heterogeneous crystal nucleation starting from

the interparticle potential. The DFT approach requires some building blocks which are needed as first steps before the nucleation problem itself can be addressed: the bulk phase diagram and the fluid–solid interface. Then we focus on the critical nucleus for heterogeneous nucleation: four typical set-ups (motivated by experiment) will be discussed, using different types of confining walls, inhomogeneous grains or nucleation seeds. Section 3 is concluded by an example, namely by a DFT-based study on heterogeneous nucleation in a two-dimensional dipolar system. In section 4 we establish a relation between DDFT and the concept of the PFC model. This paper is closed with concluding remarks.

2. Classical density functional theory

2.1. Static density functional theory

Classical density functional theory (DFT) can be viewed as a reformulation of statistical mechanics in terms of functionals and correlation functions. The central entities of this concept are the one-particle density, $\rho(\mathbf{r})$, and the Helmholtz free energy functional, $\mathcal{F}[\rho]$. In the following we briefly outline the formalism.

We consider a system of particles confined in a volume V, which is in contact with a heat and particle reservoir, specified by a temperature T and a chemical potential μ. Further, the system is under the influence of an external one-particle potential, $V_{ext}(\mathbf{r})$. $\rho(\mathbf{r})$ is defined as a grand-canonical ensemble average:

$$\rho(\mathbf{r}) = \left\langle \sum_i \delta(\mathbf{r} - \mathbf{r}_i) \right\rangle, \qquad (1)$$

where $\mathbf{r}_i$ denotes the particle positions.

It is rather easy to show that $\rho(\mathbf{r})$ is uniquely defined by $V_{ext}(\mathbf{r})$. However, the opposite statement is also true, a fact which is less obvious: a given *equilibrium* one-particle density, $\rho_0(\mathbf{r})$, also determines in a unique way the external potential $V_{ext}(\mathbf{r})$; for the proof of this remarkable property, we refer to [6].

All thermodynamic properties of the system can be obtained from the grand potential, $\Omega = \Omega[\rho_0]$, which is a functional of $\rho_0(\mathbf{r})$, i.e.

$$\Omega[\rho_0] = \mathcal{F}[\rho_0] + \int d\mathbf{r} \, [V_{ext}(\mathbf{r}) - \mu]\rho_0(\mathbf{r}), \qquad (2)$$

introducing the Helmholtz free energy functional, $\mathcal{F}[\rho_0]$. Taking into account the above remarks, both $\Omega[\rho_0]$ and $\mathcal{F}[\rho_0]$ are unique functionals of $\rho_0(\mathbf{r})$.

If we now consider Ω as defined in (2) as a functional for a one-particle density $\rho(\mathbf{r})$, which is not necessarily the equilibrium density, $\rho_0(\mathbf{r})$, then a further important property of $\Omega[\rho]$ can be derived, namely

$$\Omega[\rho] \geqslant \Omega[\rho_0]; \qquad (3)$$

in addition, the equal sign holds only if $\rho(\mathbf{r}) = \rho_0(\mathbf{r})$. Since $\rho_0(\mathbf{r})$ obviously minimizes $\Omega[\rho]$, the equilibrium one-particle density can be determined from either of the following

equations:

$$\left. \frac{\delta\Omega[\rho]}{\delta\rho(\mathbf{r})} \right|_{\rho=\rho_0} = 0 \qquad \text{or} \qquad \left. \frac{\delta\mathcal{F}[\rho]}{\delta\rho(\mathbf{r})} \right|_{\rho=\rho_0} + V_{ext}(\mathbf{r}) - \mu = 0; \qquad (4)$$

the respective first terms represent functional derivatives.

The Helmholtz free energy functional can conveniently be split into an ideal ('id') and an excess ('ex') contribution, i.e. $\mathcal{F}[\rho] = \mathcal{F}_{id}[\rho] + \mathcal{F}_{ex}[\rho]$. The first term is given by

$$\mathcal{F}_{id}[\rho] = k_B T \int d\mathbf{r}\rho(\mathbf{r})\{\ln[\rho(\mathbf{r})\Lambda^3] - 1\}; \qquad (5)$$

here k_B is Boltzmann's constant and Λ is the de Broglie wavelength. For obvious reasons, $\mathcal{F}[\rho]$ and $\Omega[\rho]$ provide full information about the thermodynamic properties of the system. In addition, via suitable functional derivatives of $\mathcal{F}_{ex}[\rho]$, the hierarchy of direct correlation functions, $c^{(n)}(\mathbf{r}_1, \ldots, \mathbf{r}_n)$, can be generated, which provides full information about the structural properties of the system:

$$c^{(n)}(\mathbf{r}_1, \ldots, \mathbf{r}_n) = -\beta \left. \frac{\delta^n \mathcal{F}_{ex}[\rho]}{\delta\rho(\mathbf{r}_1)\cdots\delta\rho(\mathbf{r}_n)} \right|_{\rho_0=\rho} \qquad (6)$$

with $\beta = 1/(k_B T)$. For $n = 2$ and taking the limit of a spatially *homogeneous* one-particle density (i.e. $\rho(\mathbf{r}) \to \rho = \text{const.}$), $c^{(2)}(\mathbf{r}_1, \mathbf{r}_2)$ becomes the Ornstein–Zernike direct correlation function, $c(r)$ [20].

2.2. Approximations

Apart from a few rather (academic) systems, no *exact* expressions for $\mathcal{F}_{ex}[\rho]$ are available. Thus one is forced to resort to approximate approaches. The most commonly used approaches are perturbative and mapping schemes. Within the class of perturbative approaches, we highlight the pioneering work of Ramakrishnan and Yussouff [21] who proposed to expand $\mathcal{F}_{ex}[\rho]$ in a functional Taylor series around the density of a homogeneous reference fluid; the expansion functions are the direct correlation functions of the homogeneous system. Usually this expansion is truncated at second order. The other class of approaches, the so-called mapping schemes, were introduced in the 1980s [22–27] where the non-uniform system, characterized by the one-particle density $\rho(\mathbf{r})$, is locally mapped onto a uniform fluid of an effective density, $\bar{\rho}(\mathbf{r})$, introducing some weight function $w(\mathbf{r})$. This category of approximate schemes includes approaches such as weighted density or modified weighted density approximations. The function $w(\mathbf{r})$ is related via nonlinear differential equations to the direct correlation functions of the homogeneous system. For an overview we refer to [6]. So far, all these schemes are general enough to be applicable to systems with arbitrary interactions.

Practical applications have revealed that particular approximate approaches have proven to be highly successful for well-defined categories of systems. We start with the fundamental measure theory proposed by Rosenfeld [28] and later in an equivalent form by Kierlik and Rosinberg [29, 30]. This weighted density approach that was originally derived for hard spheres but which has proven to be highly appropriate

for even more complex hard-core systems (for an overview see [31], for a more accurate extension of Rosenfeld's functional see, for instance, [32]). For the topic addressed in this contribution the existence of an accurate density functional $\mathcal{F}_{ex}[\rho]$ for this system is of particular relevance since hard spheres represent either a suitable potential for a certain class of colloidal particles or can be used as a convenient reference system in more complex (effective) interactions.

Another important class of soft matter systems are those which are characterized by (effective) soft or ultra-soft interactions, $\Phi(r)$, specified via $\int_0^\infty r^2 \, dr \, \Phi(r) < \infty$. Here, it has been shown [33–38] that a mean field (MF) type of functional, i.e.

$$\mathcal{F}_{ex}[\rho] = \tfrac{1}{2} \int d\mathbf{r} \, d\mathbf{r}' \rho(\mathbf{r}) \Phi(|\mathbf{r} - \mathbf{r}'|) \rho(\mathbf{r}') \qquad (7)$$

is more appropriate. It can even be demonstrated that this functional becomes more accurate as the density grows.

2.3. Dynamic density functional theory (DDFT)

We now discuss the dynamical extension of density functional theory towards Brownian dynamics which is appropriate for colloidal particles. The overdamped dynamics of a set of N identical, spherical, colloidal particles, immersed in a solvent, which serves for damping and as a heat bath, is set by the Langevin equations. Provided there are no hydrodynamic interactions between the particles, these equations are as follows:

$$\dot{\mathbf{r}}_i = \gamma^{-1}(\mathbf{F}_i + \mathbf{f}_i), \qquad i = 1, \dots, N. \qquad (8)$$

Here, the dot denotes a time derivative and $\gamma = 3\pi\eta_0\sigma$ is the friction coefficient for a sphere of diameter σ in a solvent of shear viscosity η_0. The deterministic force acting on particle i is arising from an external potential $V_{ext}(\mathbf{r}_i, t)$ and a pairwise additive interparticle potential $\Phi(|\mathbf{r}_i - \mathbf{r}_j|)$. The forces $\mathbf{f}_i$ originate from the solvent and are Gaussian white noise terms, the second moment of which is fixed by the thermal energy $k_B T$. The set of coupled, stochastic differential equations (8) for the particle coordinates is stochastically equivalent to a deterministic evolution equation for the N-particle probability density $W(\{\mathbf{r}\}, t)$, known as the Smoluchowski equation [39, 40]. This equation can be exactly integrated to obtain an exact equation for the time-dependent one-particle density field $\rho(\mathbf{r}, t)$ [41]. The averaged equation still involves a density pair correlation in non-equilibrium $\rho^{(2)}(\mathbf{r}, \mathbf{r}', t)$ which can be approximated by a yet unspecified equilibrium two-particle density correlation $\rho_0^{(2)}(\mathbf{r}, \mathbf{r}')$; the latter is evaluated at a corresponding equilibrium fluid, in which the equilibrium density $\rho_0(\mathbf{r})$ is equal to the instantaneous one-particle density $\rho(\mathbf{r}, t)$ of the non-equilibrium system. This replacement is called an *adiabatic* approximation. As a result [41], the adiabatic approximation leads to the following deterministic equation for the time evolution of the one-particle density $\rho(\mathbf{r}, t)$:

$$\dot{\rho}(\mathbf{r}, t) = \gamma^{-1} \nabla \cdot \left[\rho(\mathbf{r}, t) \nabla \frac{\delta \mathcal{F}[\rho(\mathbf{r}, t)]}{\delta \rho(\mathbf{r}, t)} \right]. \qquad (9)$$

This equation is the cornerstone of dynamical density functional theory (DDFT) as it connects the continuity equation of the density [42] to the microscopic equilibrium density functional.

In practice, the basic approximations in DDFT involve both the fundamental underlying adiabatic approximation and a concrete approximation of the static density functional. For a hard-rod fluid, the functional is known exactly and hence the adiabatic approximation can be tested in its bare bones [43]. Finally, if the dynamics of the colloids is governed by hydrodynamic interactions extra terms are needed to incorporate those [44]. Orientational degrees of freedom can also be cast into the DDFT form revealing non-trivial translational–rotational-coupling terms [45]. We emphasize that, as it stands here, the DDFT has no additional noise term. The relevance of noise is discussed, for example, in [46, 47].

3. From interparticle interactions to heterogeneous nucleation

3.1. The concept

3.1.1. Prerequisites to study heterogeneous nucleation.

Interparticle potential. The system is specified by its interparticle potential, $\Phi(r)$; we restrict ourselves to radially symmetric interactions. For colloidal particles, $\Phi(r)$ represents an *effective* interaction, where both the degrees of freedom of the hundreds or thousands of constituent particles and of the countless solvent particles have been traced out via suitable averaging methods (see, e.g., [48]). Often these effective interactions can be approximated rather accurately by model potentials, such as hard-sphere, hard-core Yukawa or dipole–dipole interactions. Also for the case of liquid metals, effective interactions can be deduced by averaging over the degrees of freedom of the electrons; they differ in their shape substantially from those of colloidal particles (see, e.g., [49]).

Bulk phase diagram. Based on these interactions, the bulk phase diagram of the system can be calculated. For the disordered gas and fluid phases a large variety of reliable liquid state theories is available [20]. The thermodynamic properties of the ordered solid phase(s), on the other hand, can be readily evaluated via a DFT-based approach as outlined in section 2.1 and using one of the approximate schemes presented in section 2.2. In an effort to describe the properties of the ordered phase(s), the one-particle density $\rho(\mathbf{r})$ is assumed to be a superposition of Gaussian density peaks located at the lattice points of a candidate structure. In case these lattices are not known *a priori*, they can be identified among all possible lattices in a free minimization procedure. In this context, genetic-algorithm-based optimization techniques have turned out to be highly successful both in hard [50, 51] as well as in soft matter systems [52].

The fluid–solid interface. At solid–fluid coexistence, the structure and free energy of the fluid–solid interface and its anisotropy with respect to crystal orientation will be obtained by free minimization of the density functional. While for hard
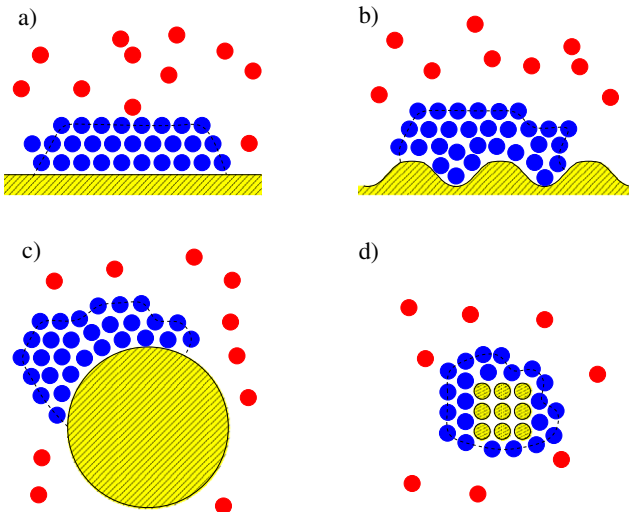
Figure 1. Schematic plots of the four different set-ups for heterogeneous nucleation discussed in this contribution: (a) a crystal nucleus near a smooth wall, (b) a crystal nucleus near a structured wall, (c) a crystal nucleus close to a large spherical particle and (d) a nucleus close to a set-up of fixed particles; the fixed particles are indicated by full circles. The nucleus is indicated by the broken line.

spheres this problem has been solved recently [53], this topic has not been addressed for soft and metallic systems. DFT-based results can readily be compared to data obtained via thermodynamic theories, such as Spaepen's expression [54], and to existing simulation data (see, e.g., [55]). In case a wall is established by an external potential acting on the system, wall–fluid and wall–solid interfacial free energies have to be considered. They can be treated within DFT and results can be compared to simulation studies (e.g. [56] for hard-sphere solids and liquids near hard walls).

3.1.2. The critical nucleus for heterogeneous nucleation.
In an undercooled or compressed fluid which is exposed to an external potential, the microscopic one-particle density distribution $\rho_c(\mathbf{r})$ of the critical nucleus for heterogeneous nucleation can be found by a search for a saddle point in the static density functional [57] by imposing a boundary condition to the minimization. This field represents a statistical average of all typical configurations. In the following we discuss in more detail four typical set-ups for the formation of the critical nucleus; they are schematically represented in figure 1.

The four different set-ups for heterogeneous nucleation are as follows:

(a) Heterogeneous nucleation near a smooth planar system wall (cf figure 1(a)): the system wall is modeled via an external potential $V_{\text{ext}}(z)$ depending on a single spatial coordinate z perpendicular to the wall. An example is a laterally integrated Lennard-Jones potential, i.e.

$$V_{\text{ext}}(z) = V_0 \left[\left(\frac{\sigma}{z} \right)^9 - \left(\frac{\sigma}{z} \right)^3 \right]. \qquad (10)$$

As far as thermodynamic variables are concerned, different distances relative to bulk solid–fluid coexistence

can be considered. In this case, the critical nucleus will have two different moments of inertia on average, one corresponding to the z axis as principal axis and another one perpendicular to it. For this set-up, DFT results can also be compared to classical nucleation theory. Furthermore, based upon the microscopic density profile $\rho_c(\mathbf{r})$ of the critical nucleus, it can be verified whether and how the concept of the contact angle is justified on a micro-scale.

(b) Heterogeneous nucleation near a periodically structured planar system wall (cf figure 1(b)): the previous set-up can be extended to the case of a *periodic* external potential, $V_{\text{ext}}(\mathbf{r})$: either via a one-dimensional periodic substructure on the wall, i.e. $V_{\text{ext}}(\mathbf{r}) = V_{\text{ext}}(z, x)$, or via a full two-dimensional lateral periodicity where a two-dimensional array of fixed particles is considered. In the experimental counterpart, such a set-up can be realized by the use of optical tweezers. In this set-up the wall structure plays a central role: depending on the specific structure and on the shape of the potential it has a distinct influence on the critical nucleus and is thus able to inhibit or accelerate heterogeneous nucleation. Further, the competition between the nucleus and substrate structure will largely influence the nucleation rates.

(c) Heterogeneous nucleation around a large spherical particle (cf figure 1(c)): in this set-up, the external potential $V_{\text{ext}}(r)$ is radially symmetric. Again, a typical example is the shifted Lennard-Jones potential, i.e.

$$V_{\text{ext}}(r) = V_0 \left[\left(\frac{\sigma}{|\mathbf{r} - \mathbf{r_0}|} \right)^{12} - \left(\frac{\sigma}{|\mathbf{r} - \mathbf{r_0}|} \right)^6 \right]. \qquad (11)$$

The size of the particle as well as the explicit form of $V_{\text{ext}}(r)$ have a distinct influence on the nucleation process.

(d) Heterogeneous nucleation around a set-up of fixed particles (cf figure 1(d)): generalizing example (c), an external nucleation seed of fixed particles is considered. This set-up is motivated by recent real-space experiments on colloids [58]. Here the variety of problems and questions to be addressed is even broader: how does a given symmetry of the fixed particle cluster steer the resulting growing crystal? Is it possible to generate a quasicrystal if the starting germ has a fivefold symmetry? How is the nucleation rate affected by the mismatch of solid structure between the seed and the thermodynamically stable crystalline phase?

3.1.3. DDFT for subsequent microstructure formation. Once the density field of the critical nucleus is determined, it can be used together with a small added noise contribution as a starting density profile for further dynamical evolution. DDFT allows for a deterministic expression of the time development of the density profile. This profile contains in principle any information about the solid microstructure and includes elastic deformation, vacancies and anisotropies across the solid–fluid interface. The second-order integro-differential equation (9) can be solved numerically by an iterative scheme. Typical ranges of time windows which are accessible on
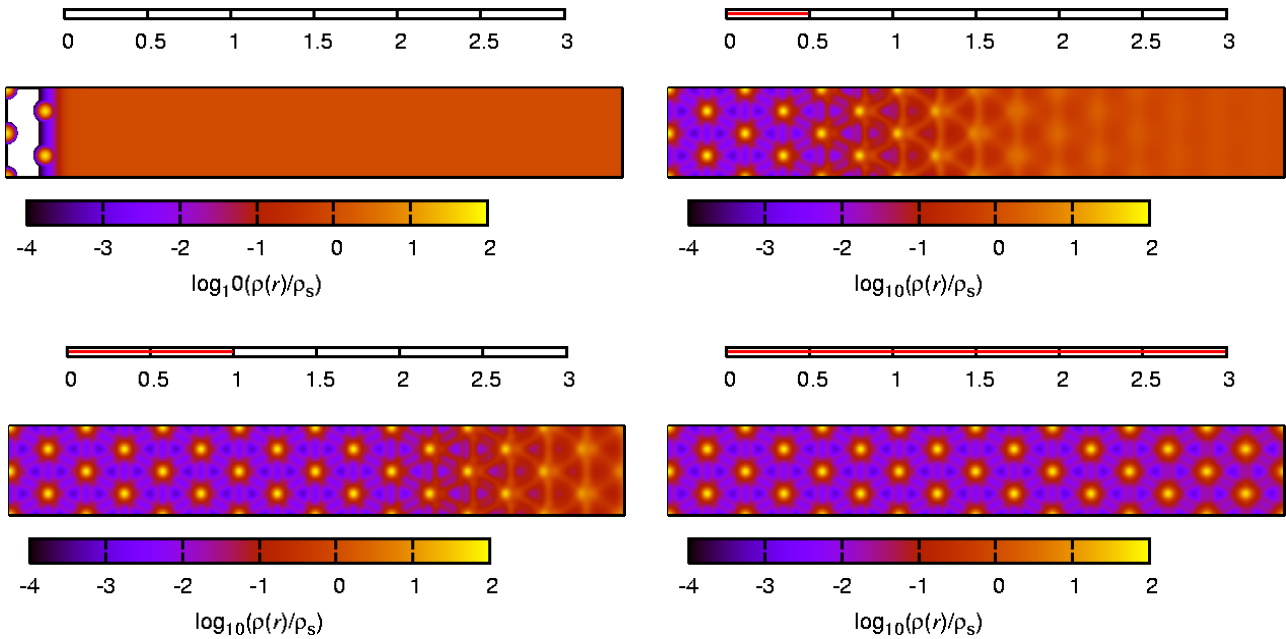
Figure 2. Four snapshots of a two-dimensional density configuration $\rho(\mathbf{r}, t)/\rho$ at times $t/\tau_B = 0, 0.5, 1.0, 3.0$ (with τ_B denoting a the Brownian timescale of the colloidal particles) after offering a nucleus to an infinite undercooled liquid at time $t = 0$, where the nucleus consists of three infinite rows of Gauss peaks. The left/right half of a rectangular periodic box with $L_x/L_y = 8\sqrt{3}$ comprises 64 particles. Note the logarithmic color scale.

present-day computers are 10–50 τ_B, where τ_B is a typical particle Brownian timescale. This allows for observation of the dynamical formation of several crystalline sheets and is ample enough to observe the crossover from post-nucleation dynamics to steady-state crystal growth. In section 3.2 we present results of a test case for such investigations.

3.1.4. DDFT for heterogeneous nucleation. A more ambitious microscopic approach to heterogeneous nucleation is to solve the DDFT together with thermal noise on it. The role of noise has recently been investigated within the framework of DDFT [46] but certainly more fundamental work is needed in this direction to clarify the role of fluctuations in the mean-field-like density functional theories. However, unlike in the umbrella-sampling technique, only small free energy barriers will really lead to a nucleation event. But the challenging question is whether even in this case a microscopic theory for the heterogeneous nucleation rate can be established.

3.2. Heterogeneous nucleation in two-dimensional dipolar systems: a test case

The general research outline described in section 3.1 was completely followed for a special simple test case, namely a one-component system of two-dimensional dipoles with a purely repulsive inverse-power-law interaction potential. This one-component system exhibits a freezing transition from a fluid into a two-dimensional hexagonal crystal. The equilibrium density functional was approximated by the traditional (and simplest) Ramakrishnan–Yussoff expression [21] which provides a reasonable description of the bulk phase diagram [59, 60]. The dynamical density functional theory

was solved numerically on a fine grid in two spatial dimensions and was applied to a variety of nucleation and crystal growth problems [47, 61, 62].

A *linear array* of fixed particles is shown in figure 2. This corresponds to the set-up (b) proposed in figure 1 for the special case that the wall structure is made up by fixed but otherwise identical particles. The initial density profile consists of two layers of crystalline particles modeled as sharp delta peaks. They serve as an external nucleus for subsequent crystal growth. After a quick relaxation of the density fields in the neighborhood of the imposed nucleation array, a crystalline front is growing until the whole box is filled with crystal.

Furthermore, in [62], an externally imposed heterogeneous nucleation cluster of fixed particles with *hexagonal geometry* was offered to a fluid system. Whether there is subsequent crystallization depends on both the spacing of the particles and the total number of fixed particles. This shows that structural details of the nucleation cluster are important. Moreover, the dynamical density functional theory was compared against Brownian dynamics simulations and qualitative agreement was found.

In conclusion, the whole scenario of heterogeneous nucleation was calculated with DDFT for a two-dimensional dipolar system in agreement with simulations. This is promising as one may expect that more complex and complicated nucleation problems in three-dimensional and/or two-component systems can be described by DDFT as well.

4. Relation to the phase field crystal (PFC) model

The phase field crystal (PFC) model is more coarse-grained than dynamical density functional theory. Typically it starts

with a phenomenological free energy functional $\mathcal{F}[\psi(\mathbf{r}, t)]$ of a phase field $\psi(\mathbf{r}, t)$ and a dynamical equation for the phase field's time evolution similar to the DDFT equation [17, 18]:

$$\dot{\psi}(\mathbf{r}, t) = D\rho\nabla^2[\psi(\mathbf{r}, t) - \tfrac{1}{2}\psi(\mathbf{r}, t)^2 + \tfrac{1}{3}\psi(\mathbf{r}, t)^3$$
$$+ (k_B T)^{-1}V_{\text{ext}}(\mathbf{r}, t) - \rho(\hat{C}_0 - \hat{C}_2\nabla^2 + \hat{C}_4\nabla^4)\psi(\mathbf{r}, t)], \quad (12)$$

where $\hat{C}_0$, $\hat{C}_2$ and $\hat{C}_4$ are phenomenological prefactors. As a special case, one may set $\mathcal{F}[\psi(\mathbf{r}, t)]$ equal to an approximative Helmholtz free energy density functional [63]. Then the phase field is interpreted as the density field, i.e. $\psi(\mathbf{r}, t) = \rho(\mathbf{r}, t)$. Recently [47] it was shown that the commonly used PFC equation [17, 18] can be derived from DDFT under an additional gradient approximation [64–66] in the order parameter and a so-called 'constant mobility approximation'. While the former is inherent in order to get any local theory, the latter can be avoided leading to a better-justified variant of the traditional phase field crystal model [47] which is as follows:

$$\dot{\rho}(\mathbf{r}, t) = D\nabla^2\rho(\mathbf{r}, t) + D\nabla \cdot \{\rho(\mathbf{r}, t)\nabla[(k_B T)^{-1}V(\mathbf{r}, t)$$
$$- (\hat{C}_0 - \hat{C}_2\nabla^2 + \hat{C}_4\nabla^4)\rho(\mathbf{r}, t)]\}. \quad (13)$$

Both phase-field-crystal approaches were tested against for a two-dimensional dipolar system [47]. In particular, the front crystal growth velocity of a two-dimensional solid into the melt at an imposed linear array of fixed particles (see again in figure 2) was calculated. Although the phase field crystal models predict wider interfaces as compared to the DDFT, in general reasonable agreement was found between the full DDFT data and the phase-field-crystal models provided a suitable scaling was performed needing to match the bulk phase diagram. As expected, the new variant proposed in [47] has a slightly better performance than the traditional phase-field-crystal model.

5. Conclusion

In conclusion, classical density functional theory provides an ideal theoretical tool to describe crystal nucleation and growth phenomena for colloidal systems whose dynamics is Brownian. The theory is microscopic, i.e. it works with the basic underlying interactions as an input and predicts the time-dependent density fields as an output. In particular, an external potential can directly be incorporated into the density functional approach which make it a versatile tool for heterogeneous nucleation. The nucleation and growth behavior at different imposed nucleation seeds have been calculated for one-component two-dimensional dipolar systems which are realized by superparamagnetic colloids at a pending air–water interface [67]. *Qualitative but not quantitative agreement* was found with Brownian dynamics computer simulations [62]. In particular the asymmetry in the parameter space for which crystal growth was found is confirmed by Brownian dynamics simulations (cf figure 3 in [62]). These results also provided a testing ground for more phenomenological phase-field-crystal models.

Future research should focus on three-dimensional and binary systems. Examples include the binary mixture of two-dimensional dipoles which exhibits a rich equilibrium phase behavior [68–70] and the three-dimensional Asakura–Oosawa–Vrij model for colloid–polymer mixtures which has been studied extensively near walls [71, 72]. For the former a Ramakrishnan–Yussoff approximation for the density functional can be employed [59, 60] while for the latter a Rosenfeld-like approximation is known [73, 74]. The results can be tested against computer simulations [75] and real-space experiments [76] on three-dimensional colloidal dispersions.

Once the critical nucleus for heterogeneous nucleation is determined and is thus known on the full microscopic scale, the following questions can be answered directly:

 (i) What is the size and shape of the critical nucleus? In particular, how anisotropic is the critical nucleus for a given external potential acting as a source for heterogeneous nucleation?
 (ii) Is the crystalline structure inside the critical nucleus the same as that for the stable solid phase?
(iii) How broad and diffuse is the fluid–solid interface of the critical nucleus? Is there an elastic distortion of the interface?
(iv) What is the free energy barrier ΔG^* of the critical nucleus? Is it larger or smaller than that for homogeneous nucleation? This gives insight into the nucleation rate which scales as $\exp(-\Delta G^*/k_B T)$, where $k_B T$ is the thermal energy.

Even more ambitious is the treatment of metallic alloys [19] within density functional theory. For the equilibrium phase diagram one may think about using an effective pair potential for the force field and employing a hard-sphere perturbation approach for the density functional combined with a mean-field theory. The dynamics of metals, however, is undamped and it is a great challenge to generalize the DDFT approach towards Newtonian dynamics. Although the first progress has been achieved here [77], the DDFT is much less advanced for molecular dynamics when compared to completely overdamped Brownian dynamics.

Acknowledgments

References

[1] Wiener M C 2004 *Methods* **34** 364
[2] Snell E H and Helliwell J R 2005 *Rep. Prog. Phys.* **68** 799
[3] Dziomkina N V and Vansco G J 2005 *Soft Matter* **1** 265
[4] Emmerich H, Binder K and Nestler B 2007 *Phil. Mag. Lett.* **87** 265
[5] Singh Y 1991 *Phys. Rep.* **207** 351
[6] Evans R 1992 *Fundamentals of Inhomogeneous Fluids* ed D Henderson (New York: Dekker)

[7] Evans R 1990 *J. Phys.: Condens. Matter* **2** 8989
[8] Ohnesorge R, Löwen H and Wagner H 1991 *Phys. Rev.* A **43** 2870
[9] Oxtoby D W and Evans R 1988 *J. Chem. Phys.* **89** 7521
[10] Athreya B P, Goldenfeld N, Dantzig J A, Greenwood M and Provatas N 2007 *Phys. Rev.* E **76** 056706
[11] Wu K A and Karma A 2007 *Phys. Rev.* **76** 184107
[12] Goldenfeld N, Athreya B P and Dantzig J A 2005 *Phys. Rev.* E **72** 020601 (R)
[13] Emmerich H and Siquieri R 2006 *J. Phys.: Condens. Matter* **18** 11121
[14] Gránásy L, Pusztai T and Warren J A 2004 *J. Phys.: Condens. Matter* **16** R1205
[15] Gránásy L, Pusztai T and Börzsönyi T 2006 *J. Mater. Res.* **21** 309
[16] Gránásy L, Pusztai T, Saylor D and Warren J A 2007 *Phys. Rev. Lett.* **98** 035703
[17] Elder K R, Katakowski M, Haataja M and Grand M 2002 *Phys. Rev. Lett.* **88** 245701
[18] Elder K R and Grant M 2004 *Phys. Rev.* E **70** 051605
[19] Emmerich H 2008 *Adv. Phys.* **57** 1
[20] Hansen J-P and McDonald I R 2006 *Theory of Simple Liquids* (Amsterdam: Academic)
[21] Ramakrishnan T V and Yussouff M 1979 *Phys. Rev.* B **19** 2775
[22] Tarazona P 1984 *Mol. Phys.* **52** 81
[23] Tarazona P and Evans R 1984 *Mol. Phys.* **52** 847
[24] Meister T F and Kroll D M 1985 *Phys. Rev.* A **31** 4055
[25] Curtin W A and Ashcroft N W 1985 *Phys. Rev.* A **31** 2909
[26] Denton A R and Ashcroft N W 1989 *Phys. Rev.* A **39** 4701
[27] Likos C N and Ashcroft N W 1993 *J. Chem. Phys.* **99** 9090
[28] Rosenfeld Y 1989 *Phys. Rev. Lett.* **63** 980
[29] Kierlik E and Rosinberg M-L 1990 *Phys. Rev.* A **42** 3382
[30] Phan S, Kierlik E, Rosinberg M-L, Bildstein B and Kahl G 1993 *Phys. Rev.* E **48** 618
[31] Schmidt M 2003 *J. Phys.: Condens. Matter* **15** S101
[32] Roth R, Evans R, Lang A and Kahl G 2002 *J. Phys.: Condens. Matter* **14** 12063
[33] Lang A, Likos C N, Watzlawek M and Löwen H 2000 *J. Phys.: Condens. Matter* **12** 5087
[34] Likos C N, Lang A, Watzlawek M and Löwen H 2001 *Phys. Rev.* E **63** 031206
[35] Archer A J and Evans R 2001 *Phys. Rev.* E **64** 041501
[36] Archer A J and Evans R 2002 *J. Phys.: Condens. Matter* **14** 1131
[37] Archer A J, Likos C N and Evans R 2002 *J. Phys.: Condens. Matter* **14** 12031
[38] Likos C N, Mladek B M, Gottwald D and Kahl G 2007 *J. Chem. Phys.* **126** 224502
[39] von Smoluchowski M 1916 *Ann. Phys., Lpz.* **353** 1103
[40] Risken H 1989 *The Fokker–Planck Equation, Methods of Solutions and Applications* 2nd edn (Berlin: Springer)
[41] Archer A J and Evans R 2004 *J. Chem. Phys.* **121** 4246
[42] Marconi U M B and Tarazona P 1999 *J. Chem. Phys.* **110** 8032
[43] Penna F and Tarazona P 2006 *J. Chem. Phys.* **124** 164903
[44] Rex M and Löwen H 2008 *Phys. Rev. Lett.* **101** 148302
[45] Rex M, Wensink H H and Löwen H 2007 *Phys. Rev.* E **76** 021403

[46] Archer A and Rauscher M 2004 *J. Phys. A: Math. Gen.* **37** 9325
[47] van Teeffelen S, Löwen H, Backofen R and Voigt A 2009 *Phys. Rev.* E **79** 051404
[48] Likos C N 2001 *Phys. Rep.* **348** 267
[49] Hafner J 1987 *From Hamiltonians to Phase Diagrams* (Berlin: Springer)
[50] Oganov A R and Glass C W 2008 *J. Phys.: Condens. Matter* **20** 064210
[51] Woodley S M and Catlow R 2008 *Nat. Mater.* **7** 937
[52] Gottwald D, Kahl G and Likos C N 2005 *J. Chem. Phys.* **122** 204503
[53] Warshavsky V B and Song X Y 2006 *Phys. Rev.* E **73** 031110
[54] Spaepen F 1975 *Acta Metall.* **23** 729
[55] Davidchack R L, Morris J R and Laird B B 2006 *J. Chem. Phys.* **125** 094710
[56] Heni M and Löwen H 1999 *Phys. Rev.* E **60** 7057
[57] Oxtoby D W 1991 *Liquids, Freezing and Glass Transitions* ed J-P Hansen, D Levesque and J Zinn-Justin (Amsterdam: North-Holland)
[58] Vossen D L J 2004 *PhD Thesis* Utrecht, The Netherlands, unpublished
[59] van Teeffelen S, Löwen H and Likos C N 2008 *J. Phys.: Condens. Matter* **20** 404217
[60] van Teeffelen S, Likos C N, Hoffmann N and Löwen H 2006 *Europhys. Lett.* **75** 583
[61] Löwen H, Likos C N, Assoud L, Blaak R and van Teeffelen S 2007 *Phil. Mag. Lett.* **87** 847
[62] van Teeffelen S, Likos C N and Löwen H 2008 *Phys. Rev. Lett.* **100** 108302
[63] Elder K R, Provatas N, Berry J, Stefanovic P and Grant M 2007 *Phys. Rev.* B **75** 064107
[64] Löwen H, Beier T and Wagner H 1989 *Europhys. Lett.* **9** 791
[65] Löwen H, Beier T and Wagner H 1990 *Z. Phys.* B **79** 109
[66] Lutsko J F 2006 *Physica* A **366** 229
[67] Zahn K, Méndez-Alcaraz J M and Maret G 1997 *Phys. Rev. Lett.* **79** 175
[68] Assoud L, Messina R and Löwen H 2007 *Europhys. Lett.* **80** 48001
[69] Fornleitner J, Lo Verso F, Kahl G and Likos C N 2008 *Soft Matter* **4** 480
[70] Fornleitner J, Lo Verso F, Kahl G and Likos C N 2009 *Langmuir* **25** 7836
[71] Wessels P P F, Schmidt M and Löwen H 2004 *J. Phys.: Condens. Matter* **16** L1
[72] Binder K, Horbach J, Vink R L C and De Virgiliis A 2008 *Soft Matter* **4** 1555
[73] Schmidt M, Löwen H, Brader J M and Evans R 2000 *Phys. Rev. Lett.* **85** 1934
[74] Schmidt M, Löwen H, Brader J M and Evans R 2002 *J. Phys.: Condens. Matter* **14** 9353
[75] Auer S and Frenkel D 2005 *Adv. Polym. Sci.* **173** 149
[76] Gasser U, Weeks E R, Schofield A, Pusey P N and Weitz D A 2001 *Science* **292** 258
[77] Marconi U M B, Tarazona P, Cecconi F and Melchionna S 2008 *J. Phys.: Condens. Matter* **20** 494233